

DIAGNOSIS OF ERODIBLE LOCATIONS IN RIVER BENDS USING A COMBINED METHOD (GIS, RS AND THE CCHE2D MODEL) (CASE STUDY: THE KARKHEH RIVER IN IRAN)

Arash ADIB^{1*}, Hamid Reza GAFOURI¹, Ali LIAGHAT¹

Abstract

In this research, a combined method was developed to determine the erodibility of bends in the Karkheh River. For this purpose, a 40 km reach of the Karkheh River downstream of the Karkheh Dam was considered. The value of the shear stress was the calculated using the CCHE2D model. The results from the model show that in 1996 (before construction of the Karkheh dam), the length of the erodible reach was 1314 m; in 2011 (after construction of the Karkheh dam), this length was reduced to 840 m. Furthermore, the model illustrates that the location of the maximum shear stress is a function of the relative curvature (R/W) in the bends. For small values of the R/W (less than 1.5), the maximum shear stress occurs on the convex bank of a river bend. By increasing the R/W, the location of the maximum shear stress transfers to the concave bank of the river bend. Also, this location is displaced towards downstream by increasing the R/W.

Address

¹ Civil Engineering Department, Engineering Faculty, Shahid Chamran University of Ahvaz, Ahvaz, Iran

* **Corresponding author:** arashadib@scu.ac.ir

Key words

- Bends,
- GIS,
- CCHE2D model,
- The Karkheh River,
- Relative curvature.

1 INTRODUCTION

Rivers naturally undergo processes of erosion, sedimentation, and geomorphic changes. The instability of river banks and the sides of a channel can be explained by multiple causes such as the transportation of soil particles by the flow and fluvial waves, erosion occurring on the basal sides of river banks, the collapse and internal incision of the river, and increases in the slope angle due to erosion and riverbed scour. Furthermore, the instability of river banks can also be explained by pore water pressure under saturated conditions, the internal distortions of a slope angle due to water infiltration, and the erosive effects of agricultural wastewater entering the river. Generally, the stability of rivers is influenced by intrinsic parameters that are in a direct relation with the fluvial system and by external parameters such as climatic variables, vegetation, human intervention, and the mechanisms by which river icing and melting occur. The intrinsic parameters of such effects include the geomorphic structure of the river, the type of river, e.g., meandering, braided or straight, the geometric properties and hydraulic qualities of the river bends, the physical

composition of the river bed and river bank, hydraulic variables, and also the factor of shear stress. Qualitative and quantitative changes to any such intrinsic or extrinsic parameters can have measurable impacts on the stability of a river (Amiri-Tokaldany et al. 2007).

The factors involved in erosion and sedimentation events are commonly explained in scientific literature such as in van den Berg (1995), which have led to predictions regarding bed reformations and the shaping of illustrative plan forms. However, the prediction of these changes and their corresponding numerical simulations are difficult to achieve based on exact values of measurement. Nevertheless, it is still practical to observe geomorphic changes in the course of a river over a considerable span of time and consequently devise particular measures to prevent the river's instability by identifying the relevant criteria that are responsible for causing such instabilities (Yu et al. 2010).

The hydraulic analysis of a fluvial system on a river bend leads to substantial discussions regarding any alterations that are gradually made to the meanderings of the river over time and issues concerning the simulation of the flow and the changes occurring to the river

bed, which are common features of meandering rivers. In this regard, the simulation of the lateral velocity and shear stress distribution occurring in the river bend is of analytical importance and is functional with respect to preserving river banks in their appropriate forms. Such simulations are also beneficial to understanding the pattern of sediment transport and the actual sedimentation or erosion. Simulations of lateral velocity and shear stress distribution are also used in measures to design flood control methods and in the engineering of fluvial canals that help prevent flooding as in Alauddin and Tsujimoto (2012).

In straight canals, the rapid gradient and speed of the flow among the major fluvial layers and the floodplain layer can act to generate strong vortex flows along the border where the major fluvial section flanks the floodplain. The resulting effect of these vortices is the translocation of the major fluvial momentum to the floodplain. It also results in an initiation of shear stress, a decline in fluvial energy and, ultimately, a reduction in the speed and outflow of the river (Omran, 2008).

The meandering of rivers naturally result in various phenomena along their course, and some may cause problematic aspects with regard to human projects. Therefore, researchers have extensively investigated the causes and mechanisms by which meandering rivers are formed and altered in their course of progression and development. The results of such investigations reveal that multiple factors are involved in the formation and development of meandering rivers. Local features are determinant factors with respect to where the river is situated, and the type of formations and nearby installations can largely predetermine the intensity and dimensions that could be inflicted on human-made structures and installations (Rüther and Olsen, 2007; Verhaar et al. 2008).

There is a considerable gradient of change in the longitudinal distribution of fluvial speed when comparing the inner side of a bend with the outer side. Due to successive alterations in the radius of various curvatures of bends, fluvial parameters are more complex and sophisticated in meandering sections compared with straight sections (Patra et al. 2004).

Zámolyi et al. (2010) described the geometric shape of a river as a function of the outflow, sedimentation and hydraulic circumstances of the flow. However, these researchers focused on one particular factor and overlooked a systematic analysis of the geomorphic conditions and geological aspects of the river course under study.

Constantine et al. (2010) evaluated the mechanism of the cutoff formation along the course of large meanders by the topography of the floodwater. Researchers have hypothesized that sporadic changes in the capacity of river sections or the installation of natural dams and the occurrence of sudden flood surges could be causes of cutoff formations.

Güneralp and Marston (2012) assessed the stages by which morphodynamic meanders are formed. Further discussions were undertaken regarding the mechanisms by which meanders are formed through hydrodynamic forces and the geometric patterns of their transformations.

The pattern of shear stress distribution depends on factors such as the geometry of the cross section of the river, the qualities of any secondary flow, and unevenness in the bed and banks of channels. Generally, researchers have considered two methods to determine the qualities and quantities of shear stress. A first group has made use of mathematical relations and diagrams pertaining to the shear stress of material debris on the threshold of movement or transportation (Chang 1983, 1985, 1994; Chang and Stow 1989; Chang et al. 1996; Amiri-Tokaldany et al. 2007). A second group of researchers utilized information according to the results of physical models and field experiments (Wilcock, 1993; Haynes and Pender, 2007; Thoman and Niezgodna, 2008; Kean et al. 2009).

Khan et al. (2000) calculated depth-averaged velocity and water surface profiles in the main and branch channels of a bifurcating channel using the CCHE2D model. The water surface profile calculated by the model had a good fitness with the observed water surface profile. Due to the absence of field data, flume data collected in the laboratory was utilized for the channel's bifurcation and confluence to verify the simulated results.

Duan et al. (2001) analyzed variables such as velocity, depth and shear stress using the CCHE2D model and collecting data in a laboratory. The erosion of a bank, the formation and shifting of bars and pools, and the formation of meanders by the model had a good fitness with the observed phenomena.

Kim et al. (2010) determined the flow characteristics in natural channel bends of the Daeyu reach with the CCHE2D model; this reach is located downstream of the Young Dam. The results showed that in the upstream, the water level simulated by the CCHE2D model was 1.5 m higher than the water level simulated by the 1-D numerical model (HEC-RAS) because the HEC-RAS model could not consider the effects of the geometry of the bend on the flow. Also, Nassar (2011) simulated a part of the Nile River using the CCHE2D model, and Hasan et al. (2011) simulated the transport of sediment and pollutants in the Gambier River and Harapan Lake using the CCHE2D model. Jang et al. (2013) investigated the stabilization of the bed in the upstream channel of the Haman Weir by also using the CCHE2D model. The results of the studies in which the CCHE2D model was applied to calculate shear stress are a favorable base for comparison with the present study.

Brandt (2000) studied changes in the geomorphology of a river downstream of dams. He classified slope, cross-section, plan form and bed form changes and the tributary response to the main stream changes based on changes developed in the flow discharge, sediment load, and sediment transport capacity of flows by dams. Also, he considered the variability of geomorphological changes with regard to the time and distance from the reservoir.

In addition to the effects of flow discharge and sediment load changes, this research considers the effect of relative curvature on changes in the width, length and slope of a river and the shear stress in river meanders. Additionally, according to the principles stated by Ikeda and Parker (1989), Termini (2015), and Di Silvio (2009), satellite images and the CCHE2D software are utilized for identifying meanders and the calculation of shear stress in meanders.

According to the mentioned criteria, it is necessary to compare two factors for the determination of erodible sections in a river: (1) the shear stress calculated by arithmetic models, and (2) the highest level of threshold shear stress (incipient movement) with respect to the empirical data and relevant formula. The purpose of our research is to present a combined method based on the maximum allowable shear stress of incipient movement for the purpose of establishing the extent to which certain meandering rivers can be erodible. The use of a combined selection of erodibility maps and the relations between the threshold shear stress of alluvial materials with the soil texture are methods that can replace the Shields diagram and empirical formula available for the determination of threshold shear stress. Conventional erodibility maps are costly and time-consuming for determining and calculating the extent of the lateral erosion of river banks. On the contrary, applications of the Geographic Information System (GIS) and Remote Sensing (RS) are less expensive but are efficient methods for this purpose, which form the foundation of this research.

The stages of this research are:

- The determination of the location, width (W) and radius (R) of the river bends of the Karkheh River (downstream of the Karkheh dam) by GIS and satellite images;
- A comparison between the length and width of the river, the amount and geometry of the river bends in 1996 and 2011; the

- satellite images can be analyzed by GIS and RS soft ware;
- A determination of the shear stress along the river bends and identification of the reach that has the maximum shear stress by applying the CCHE2D software; and
 - Calculation of the relative curvature (R/W) of different bends and classification of the bends based on R/W.

2 MATERIALS AND METHODS

The purpose of this research is to present an integrated method based on maximum shear stress (incipient motion) in order to determine the erodibility of meandering rivers. The CCHE2D hydro-morphodynamic model was used in this research. The CCHE2D model can simulate the effects of hydraulic structures, lateral and longitudinal changes of rivers, and displacements of river bends. This model does not have any limitations for two - dimensional simulations of flow and sediment transport.

The deformations were determined along with changes in the hydraulic parameters in the river within a time span ranging from 1996 to 2011. The steps in this research were as follows:

- Calculating the hydraulic parameters of the flow (water surface profile, lateral and longitudinal speed, and shear stress) with the CCHE2D hydrodynamic model;
- Preparing a soil shear resistance map using GIS and RS;
- Comparing the shear stress calculated with the hydrodynamic model and illustrating the critical shear stress on the soil shear resistance map; and
- Determining the erodible region in which the shear stress calculated is more than the critical shear stress.

2.1 Shear velocity formulae

The CCHE2D numerical model has two methods to determine shear velocity. In the first method the logarithmic law obtained by Equation (1) is applied:

$$\frac{U}{u_*} = \frac{1}{Z} \left[\frac{Z_0}{h} - 1 + \ln \left(\frac{h}{z_0} \right) \right] \quad (1)$$

Z is distance from the bed of channel in perpendicular direction on the bed, h is the water depth and u_* is shear velocity.

Where in U is obtained from Equation (2):

$$U = \sqrt{u^2 + v^2} \quad (2)$$

u and v are longitudinal and lateral velocities, respectively. The Z_0 varies based on the various conditions of the flow (the height of the surface roughness and the cinematic viscosity of the fluid). It is calculated by Equations (3) to (6):

$$Z_0 = 0.11 \frac{v}{u_*} + 0.0333 k_s \quad 5 \leq u_* k_s / v \leq 70 \quad (3)$$

$$Z_0 = 0.0333 k_s \quad u_* k_s / v \geq 70 \quad (4)$$

$$Z_0 = 0.11 \frac{v}{u_*} \quad u_* k_s / v \leq 5 \quad (5)$$

$$\tau_{bx} = \frac{1}{8} \rho f_c u U \quad \tau_{by} = \frac{1}{8} \rho f_c v U \quad (6)$$

where K_s is the height of the bed's surface roughness, ρ is the specific gravity of water, τ_{bx} and τ_{by} are longitudinal and lateral shear stress of the river bed, respectively, and v is the cinematic viscosity of the fluid. Since u_* is implicit, Equation (6) is obtained by trial and error.

Then the Darcy–Weisbach friction factor (f_c) can be obtained when u_* is calculated.

In the second method, the velocity and shear stress of the river bed are calculated using Manning's equation:

$$\tau_{bx} = \frac{1}{h^{\frac{1}{3}}} \rho g n^2 u U \quad (7)$$

$$\tau_{by} = \frac{1}{h^{\frac{1}{3}}} \rho g n^2 v U \quad (13)$$

where n is the Manning's coefficient, and g is the gravitational acceleration.

The shear velocity can be calculated by Equation (14).

$$u_*^2 = \frac{1}{\rho} \sqrt{\tau_{bx}^2 + \tau_{by}^2} \quad (14)$$

In this research the second method is utilized. The Manning's coefficient is a local constant. Therefore, this coefficient can be considered independently of the flow conditions. In field studies for calculating shear stress in rivers, the second method is more efficient than the first and does not require large amounts of data. This method is a lump method and considers an average value for parameters such as the bed form, channel geometry, sediment size, vegetation, etc. However, for a detailed near field simulation/verification with experimental data, the first approach is physically sound and thus worth adopting if a roughness parameter is available (Jia and Wang, 2001).

2.2 The case study

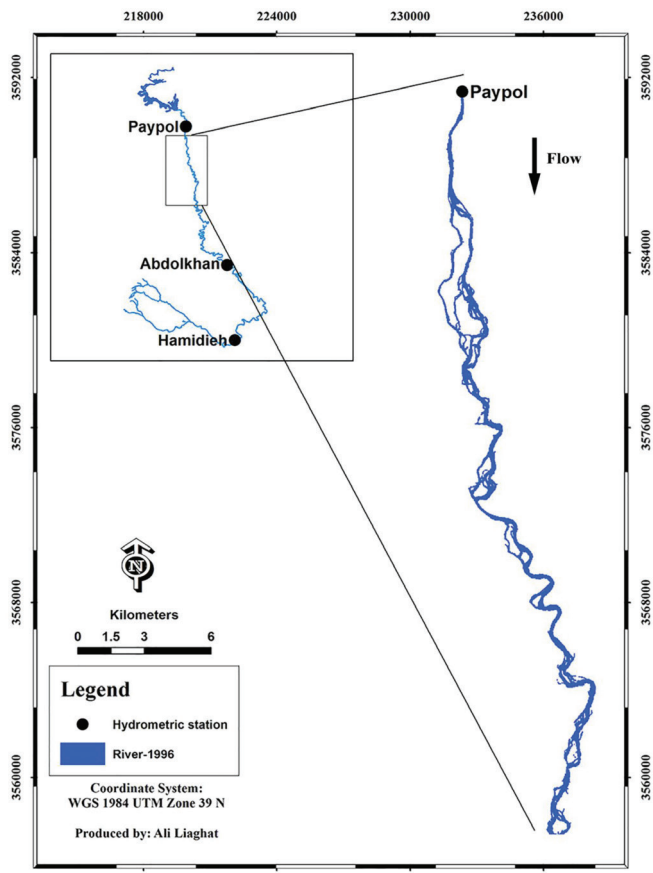
The Karkheh River (the third largest river in Iran) is located in the southwest of Iran. The source of this river is the Zagros Mountains, and it flows into the Hawr-al-Azim wetlands on the Iran-Iraq border. The length, width and depth of the river are 900 km, 30-700 m, and 4-6 m respectively. The area of its watershed is 51,481.9 km². The minimum, average and maximum heights are 3 m, 1320 m and 3645 m, respectively. The minimum, average and maximum annual temperatures are -1, 15.3 and 25.8°C. The minimum, average and maximum annual precipitation (rainfalls occur in the winter) are 205, 477 and 1000 mm. The average annual amount of potential evaporation is 2290 mm. The Karkheh Dam is the largest earth dam in Iran. Constructed in 1999, this dam is located upstream of the Pay-e-Pol hydrometric station (the distance between them is 12 kilometers). Its drainage area is 42,644 km². This dam supplies potable water and agricultural water for the Azadegan plain. Moreover, it controls large floods and generates hydroelectric power.

In order to simulate the pattern of flow for the hydraulic analysis of meanders, a reach of the Karkheh River was considered downstream of the Karkheh Dam and the Pay-e-Pol hydrometric station.

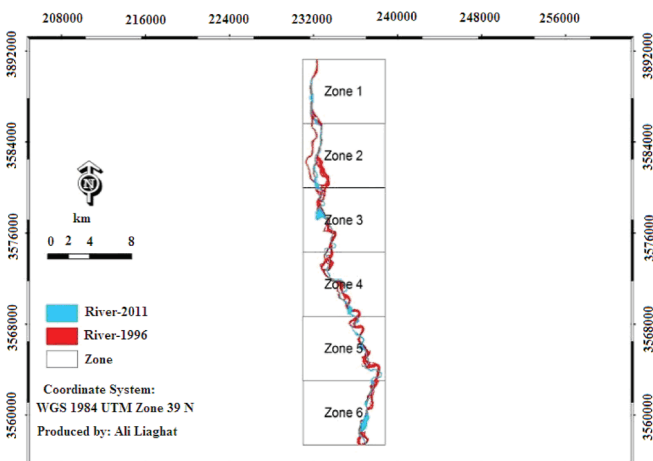
The reach selected is approximately 40 km and is divided into 6 zones. Fig. 1 illustrates the selected reach of the Karkheh River and the divisions of the reach in 1996 and 2011, i.e., before and after the construction of the dam.

2.3 Preparation of the soil shear resistance maps

Preparing a soil shear resistance map is a fundamental practice for soil management against erosion and the maintenance of rivers. However, the preparation of soil shear resistance maps is time consuming and costly if done by conventional methods (using surveying, the drilling of boreholes and sampling of soil, performance of field



(a)



(b)

Fig. 1 a) The location of the selected reach of the Karkkeh River b) the zones of the selected reach in 1996 and 2011 (before and after the construction of the dam).

and laboratory tests, and the preparation of paper maps). Alternatively, by employing GIS and RS, the preparation of maps becomes faster and more accurate (Ganasri and Ramesh, 2016). The shear resistance of the surface soil is an important feature in estimating and measuring the erodibility of soil; nevertheless, the measurement of this parameter can be costly and time-consuming if a broad area of a floodplain or basin needs to be dealt with. Therefore, applying GIS and RS techniques is necessary for this purpose. Parameters such as the vegetation, land use, type of geological installations, and direc-

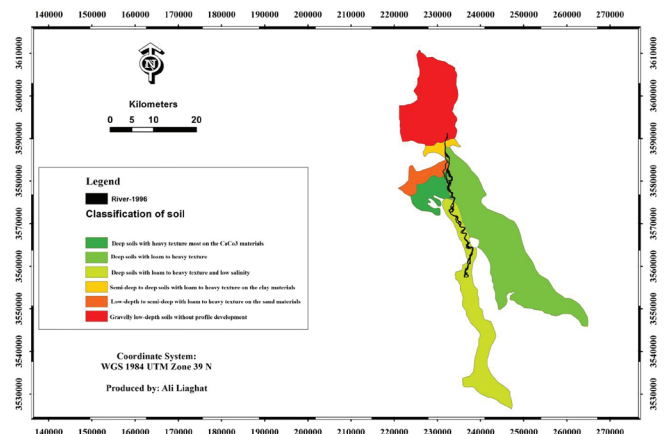


Fig. 2 Map of the alluvial classification and land use around the Karkkeh River.

tion and height of slopes are factors involved in composing a soil shear resistance map. It has been previously used in similar research (Michalik and Tekielak, 2013; Bandyopadhyay et al. 2014; Grimaud et al. 2015). Accordingly, satellite images of the Landsat 4-5 Thematic Mapper (TM) are used along with ILWIS software to obtain land use maps, while the GIS is used for the integration of the data and an analysis of the model whereby the ultimate output of the maps is achieved. In this research, small-sized particles of the alluvial content are mostly clay-silt and fine-grain sand, which results from erosion occurring in the Lahbari sector of the Aghajari formation. These sediments are characterized by weak cohesiveness and therefore show little resistance against erosion. This can lead to extensive erosion and deformations during large floods. Fig. 2 shows a map of the alluvial soil classification and land use around the Karkkeh River, which was derived using the aforementioned method.

The types of soil in the different zones around the reach of the Karkkeh River considered have been derived from Fig. 2, and data on the land use and soil resources in Khuzestan Province is presented in Tab. 1.

The erodible sectors can be distinguished by determining the critical shear stress of the soil profiles around the Karkkeh River (Tab. 2) and their subsequent comparison with the calculated shear stress of the model in the same zone.

Tab. 1 Types of soil profiles in different zones (around the Karkkeh River).

Tab. 2 Critical shear stress of different soils (Avila et al. 2014).

Zone	Type of soil profile	Material	τ (N/m ²)
1	Gravel	Fine sand, colloidal	3.60
2	Silty clay	Alluvial silts, non colloidal	7.18
3	Stiff clay	Stiff clay	22.02
4	Silty clay	Fine sand, non colloidal	3.00
5	Stiff clay	Silty clay	12.00
6	Silty clay	Alluvial silts, colloidal	22.02
		Fine gravel	15.32
		Coarse gravel	32.08
		Cobbles	52.67

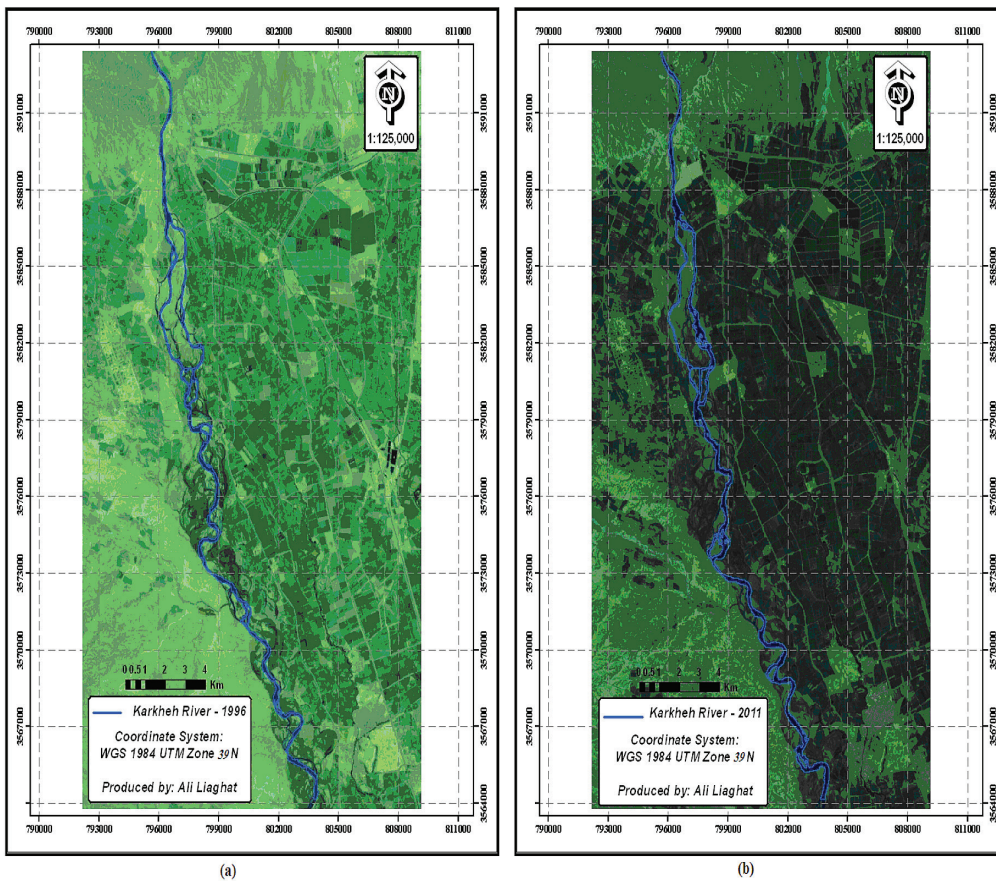


Fig. 3 The processed Landsat images by ILWIS a) 1996 and b) 2011.

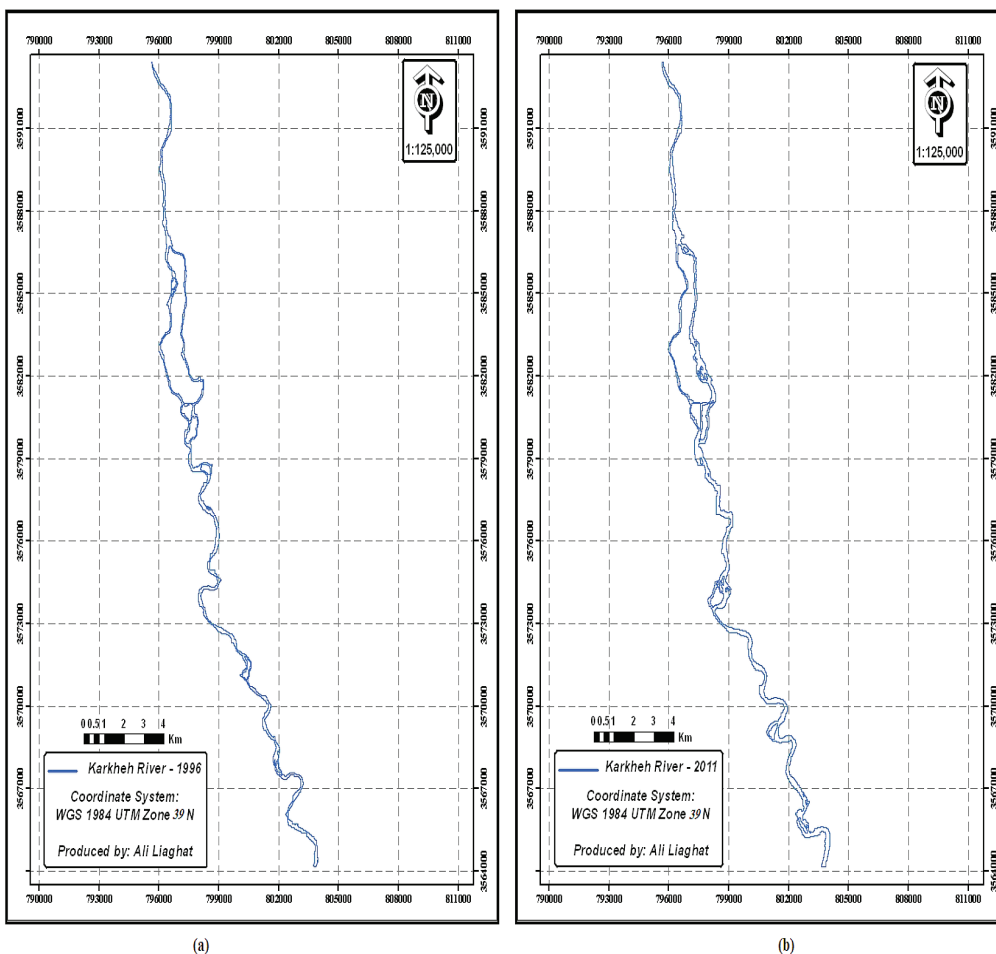
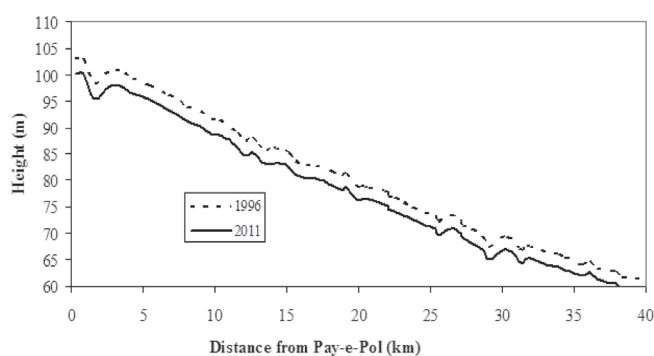


Fig. 4 The plans introduced to the CCHE2D model as geometric data a) 1996 and b) 2011.

Tab. 3 Minimum, average and maximum of the river slope in 1996 and 2011.

Year	Distance from Pay-e-Pol (km)	Minimum slope (%)	Average slope (%)	Maximum slope (%)
1996	0-10	0.011	0.153	1.831
	10-20	0.01	0.143	1.671
	20-30	0.012	0.146	1.703
	30-40	0.014	0.169	1.974
	0-40	0.0118	0.1528	1.7948
2011	0-10	0.0107	0.15	1.794
	10-20	0.0101	0.144	1.687
	20-30	0.0118	0.144	1.686
	30-40	0.0141	0.17	1.981
	0-40	0.0117	0.152	1.787

**Fig. 5** The profiles of the river bed a) 1996 b) 2011.

2.4 Introducing geometric data to the CCHE2D model

Fig. 3 illustrates Landsat images of the reach considered. These images were processed by ILWIS (RS software) and belong to the years 1996 and 2011.

By using GIS software, the processed Landsat images were converted to the plan of the reach considered. These plans (related to 1996 and 2011) were introduced to the CCHE2D model as geometric data. Fig. 4 shows these plans.

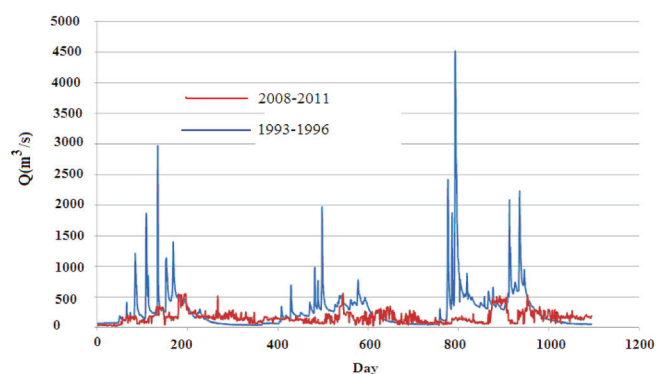
Additionally, in the reach considered, the Khuzestan Water and Power Authority (KWPA) mapped 34 cross sections in 1996 and 2011 (especially in the river bends). The minimum and maximum distances between the consecutive sections are 86 and 2318 meters.

Profiles of the river bed (in 1996 and 2011) are shown in Fig. 5.

The minimum, average and maximum of the river slope (in 1996 and 2011) are illustrated in the table below.

2.5 Introducing boundary conditions to the CCHE2D model

The long-term effects of a river flow are the most important factors that determine the erodibility of a riverbed and banks. In this research, a daily flow discharge hydrograph was considered at the Pay-e-Pol hydrometric station as the upstream boundary condition;

**Fig. 6** The daily flow discharges at the Pay-e-Pol hydrometric station.

therefore, a period of three years was provided as the model's input. The daily discharges in the years 1993 to 1996 were considered as daily flow discharges before the construction of the dam, and the daily discharges in the years 2008 to 2011 were considered as daily flow discharges after the construction of the dam. The upstream boundary conditions (in 1996 and 2011) are shown in Fig. 6. The mean and maximum daily flow discharges were 226 and 4440 m³/s in the years 1993 to 1996. Also the mean and maximum daily flow discharges were 48 and 553 m³/s in the years 2008 to 2011.

For the downstream boundary conditions, the flow discharge-stage curve is considered in the last section.

2.6 Calibration of the CCHE2D model

The Manning's coefficient of the different parts of the reach considered was determined by the calibration of the model. For this purpose, the water level calculated by the model was compared with the water level observed at the Pay-e-Pol hydrometric station. The reach considered was divided into four parts. The distances between the end of the parts and the Pay-e-Pol are 12.3, 20.1, 30.5 and 44.2 km respectively. For the calibration of the model, nine flow discharges were considered (63, 76, 252, 370, 557, 608, 1210, 2459 and 4440 m³/s in the years 1993 to 1996 and 18, 21, 37, 50.9, 106, 110, 120, 159 and 181 m³/s in the years 2008 to 2011). The calibrated Manning's coefficients (in 1993- 1996 and 2008- 2011) are 0.039- 0.042 for 0 – 10 km

Tab. 4 The results of the calibration of the CCHE2D model.

Year	Maximum relative error (%)	Maximum difference between calculated and observed water level (cm)	RMSE (cm)
1993- 1996	2.2	10	4.24
2008- 2011	2	4	2.02

from the Pay-e-Pol hydrometric station, 0.037 – 0.039 for 10 – 20 km from the Pay-e-Pol hydrometric station, 0.036 – 0.038 for 20 – 30 km from the Pay-e-Pol hydrometric station, and 0.034 – 0.036 for 30 – 40 km from the Pay-e-Pol hydrometric station.

The results of the model's calibration are illustrated in Tab. 4 for 1996 and 2011.

3 RESULTS

3.1 Determination of the changes in the length and width of the reach considered by the satellite images

By measuring the width and length of the river along various points on the reach of the river and by dividing the river into 6 zones, the following results were obtained:

Tab. 5 illustrates the minimum and maximum of the river's width and length and any changes in the 6 zones (from 1996 to 2011).

3.2 Calculation of the shear stress by the CCHE2D model

The soil profile of the lands that surround the river is silty clay (up to 91%) and stiff clay (7% of the profile). These soils have a high degree of resistance against erosion (Tab. 2); therefore, the length of the eroded part of the river is not long. The soil shear resistance maps and results of the numerical model confirm this assumption.

The shear stress calculated by the CCHE2D model is presented in Tab. 6. Tab. 7 shows the erodible regions around the river.

In 1996, six zones had a medium to high amount of erosion. The length of the erodible region was 1314 meters, which was nearly 3% of the total length of the reach. The eroded bank observed was divided into 67% and 33% for the eastern and western banks of the river, respectively.

In 2011, the intensity of the erosion was medium to high. The length of the erodible region was 840 meters, which is 2% of the total length of the reach. The eroded bank observed was divided into 20% and 80% for the eastern and western banks of the river, respectively. After the construction of the dam, the reduction in the flow discharge led to a decreased area and wetted perimeter of different sections of the river.

Therefore, the eroded length was reduced after the dam's construction (-36%). Fig. 7 shows the shear stress along zone 5 of the reach considered in 1996 and 2011.

In 1996, the distances between the Pay-e-Pol hydrometric station and the points that had the most noticeable amounts of erosion were 31,792, 33,505 and 33,800 m. The relative curvatures of the meander at these points were 4.58, 4.63 and 4.75, respectively.

In 2011, these distances were 25,530 and 32,860 m. The relative curvatures of the meander in these points were 4.86 and 5.01, respectively.

These points are in meanders, the relative curvatures of which are greater than those of other meanders (these points have the largest relative curvatures in the river).

Tab. 5 The minimum and maximum river widths and river lengths (in 1996 and 2011) and any changes in them from 1996 to 2011.

Zone	1996			2011			Changes from 1996 to 2011		
	Min width (m)	Max width (m)	River length (m)	Min width (m)	Max width (m)	River length (m)	Min width (m)	Max width (m)	River length (m)
1	141	903	3398	46	288	4181	-95	-615	783
2	545	1879	6622	51	350	6295	-494	-1529	-327
3	161	1038	6506	50	901	8191	-111	-137	1685
4	122	1135	8394	56	505	8312	-66	-630	-82
5	213	709	7986	62	388	8865	-151	-321	879
6	202	1151	6340	26	554	6299	-176	-597	-41
Average (m)	231	1136		49	498		-182	-638	
Sum (m)			39246			42143			2897

Tab. 6 Sample of the shear stress calculated by the CCHE2D model.

X_Coordinate (m)	Y_Coordinate (m)	X_Shear Stress (N/m ²)	Y_ShearStress (N/m ²)	Total_Shear tress (N/m ²)
229,974.06	3,583,963.02	6.694	-3.238	7.436
230,211.34	3,576,116.26	3.462	-3.053	4.616
232,513.07	3,583,437.78	-1.506	-1.662	2.243

Tab. 7 Erodible regions surrounding the river in 1996 and 2011.

Year	Zone	Distance from Pay-e-Pol station (m)	Erodible region length (m)	Max shear stress calculated by model in erodible region (N/m ²)	Eroded bank
1996	2	9,092-9,270	178	18.44	Right
	3	10,190-10,346	156	16.44	Right
	5	31,660-31,925	265	29.60	Right
	6	33,350-33,660	310	21.83	Left
	6	33,660-33,940	280	23.87	Right
	6	35,665-35,790	125	13.42	Left
	2	9,095-9,265	170	16.45	Right
2011	3	14,070-14,100	30	12.27	Left
	3	16,330-16,430	100	14.54	Left
	4	25,390-25,670	280	29.31	Left
	5	32,730-32,990	260	26.10	Left

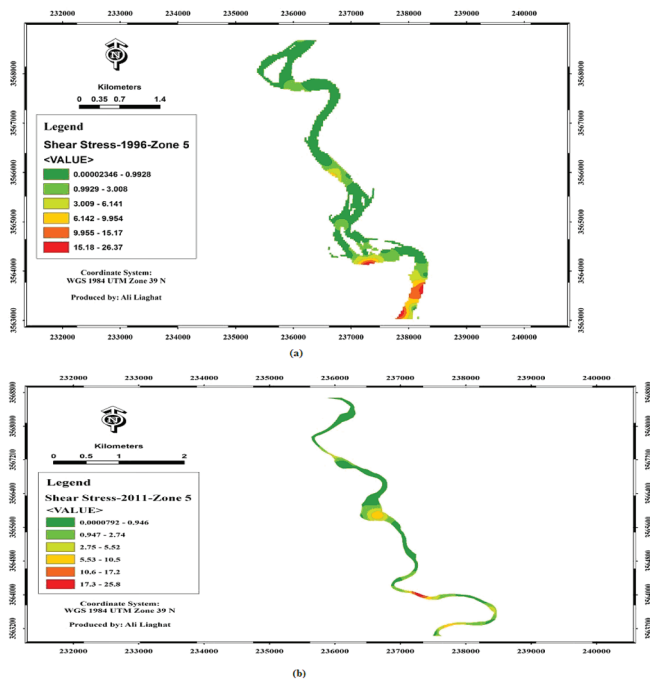


Fig. 7 Shear stress along zone 5 of the reach considered in a) 1996 b) 2011.

3.3 Relation between the location of the maximum shear stress and R/W

For determining the relation between the locations of the maximum shear stress and R/W, satellite images in 1996 and 2011 and the CCHE2D model were used. Tab. 8 and Fig. 8 show the relation between the location of the maximum shear stress and different R/Ws. In this table and figure, $\bar{\tau}$ is the mean shear stress in reach AB, and τ_0 is the shear stress at point O.

Because the water pressure in bends is slightly higher near a convex bank in comparison with a concave bank, there is a pressure

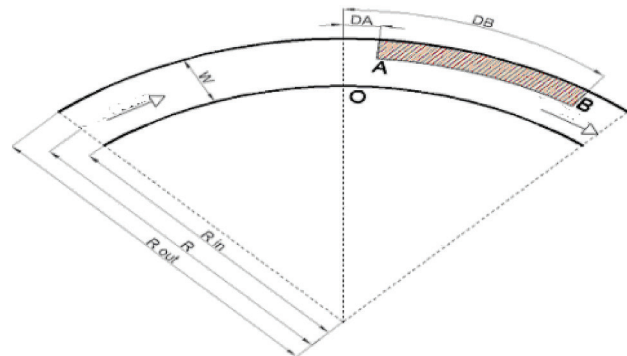


Fig. 8 Location of the maximum shear stress.

Tab. 8 Characteristics of the location of the maximum shear stress (reach AB).

R/W	Year	Number of bends	DA/W	DA/R	DB/W	DB/R	$\bar{\tau} / \tau_0$	Number of bends that maximum shear stress occurs in reach AB
R/W<1.5	1996	4	-0.56	-0.45	0.48	0.41	1.51	4
	2011	6	-0.74	-0.6	0.74	0.67	1.3	5
1.5<R/W<3.5	1996	7	1	0.5	1.6	0.8	2.2	6
	2011	10	1.42	0.69	3.25	1.41	3.23	8
3.5<R/W<5	1996	2	0.13	0.04	1.19	0.31	3.85	2
	2011	9	0.48	0.11	2.7	0.62	4.47	8
R/W>5	1996	4	1.23	0.2	1.94	0.3	2.69	4
	2011	7	5.33	0.88	7.84	1.31	7.14	6

gradient from the convex bank towards the concave bank. Therefore, centripetal force is exerted by the pressure gradient. The primary flow around the bend is a vortex flow, i.e., there is greater pressure and a slower speed near the convex bank and lower pressure and a faster speed near the concave bank. Hence the maximum shear stress and erosion occur in the concave bank of the bend.

3.4 Discussion

According to Tab. 5, the following results can be reported:

The minimum width of the river before the dam's construction was 141 meters in zone 1, while the maximum was 1879 meters in zone 2.

After the dam's construction, the minimum width of the river was 26 meters in zone 6, while the maximum was 901 meters in zone 3.

The biggest change in the river's width was observed in zone 2 (from 494 to 1529 m). This shows that zone 2 has the greatest lateral displacement.

Before the dam's construction, the maximum length of the river was 8394 meters in zone 4, and the minimum length was 3398 meters in zone 1.

After the dam's construction, the maximum length of the river was 8865 meters in zone 5, and the minimum was 4181 meters in zone 1.

The biggest change occurred in zone 3 with an increase of 1685 meters in the length of the river, while the smallest change occurred in zone 6 with a decrease of 41 meters in the length.

The soil of the river bank is silty clay in zones 2 and 6 (Tab. 1), and the critical shear stress of this type of soil is less than that of other soil types (Tab. 2). Therefore, the river's width shows the most changes in these zones. Because of a considerable decrease in the flow discharges, the river's width was significantly reduced after the dam's construction. Before and after the construction of the dam, the long-term mean annual flow discharges were equal to 369 m³/s and 351 m³/s (the change of the annual flow discharges was -5%), respectively. As can be observed, the reduction in the mean annual flow discharge is negligible. Therefore, the main cause of the reduction in the river's width is a significant reduction in the flood discharges after the dam's construction.

The greatest measured flow discharge was 600 m³/s after construction of the dam. Therefore, the water could not overflow the river banks and submerge around the floodplains. The greatest measured flood discharge was more than 5000 m³/s before construction of the dam. Therefore, the mean reduction in the minimum and maximum widths of the river was 21% and 44% respectively. The main cause of the changes in the river's width in this research is similar to that of the research by Nones et al. (2013).

The relative curvature (R/W) of the bends is less than 1.5 in zones 1, 3 and 5, and the length of the river shows the most changes in these zones. Due to the reduction in its relative curvature, the river's instability (in the plan and the longitudinal profile) has increased. After the dam's construction, the river's width (W) decreased considerably; therefore, the radius of the bend (R) decreased, while the R/W increased too. The reduction in the radius of the bend increased the length of the river bends.

On the other hand, the relative curvature of the bends is 1.5 to 3.5 in zone 2, 3.5 to 5 in zone 4, and more than 5 in zone 6. The results of the study by Brandt (2000) confirmed those changes in the river's width and length obtained by the present research.

Cramer (2012) prepared guidelines for river engineers and environmental experts in the U.S.A. He determined the location of the maximum shear stress in river bends based on different R/W s. The results of this research fit well with this guideline.

This level of fitness is 83 to 100% for $R/W < 1.5$, 80 to 86% for $1.5 < R/W < 3.5$, 89 to 100% for $3.5 < R/W < 5$, and 86 to 100% for $R/W > 5$.

4 CONCLUSION

Generally, the construction of the Karkheh Dam has considerably reduced the width of the river downstream of the dam; after the dam's construction, the minimum and maximum of the river's width reduced to 21% and 44%. From 1996 to 2011, the length of the river increased 2897 meters. The analysis shows that before the dam's construction, the sector at 30-35 kilometers downstream of the Pay-e-Pol station had the most erosion. After the dam's construction, the erodible reach progressed upstream, and this reach is between 25 km to 32 km downstream of the Pay-e-Pol station. Because of the sediment trap capacity of the dam, displacement of the erodible reach occurred. The outflow from the dam is clear water, and this flow has a high potential for erosion; therefore, parts that are close to the dam are strongly eroded. The CCHE2D model shows that the dam construction reduced the length of the erodible reach to 36%. With respect to the type of soil on the river banks (silty clay and stiff clay), it has been observed that the soil has fairly good resistance against erosion; therefore, erosion occurs only in 2% to 3% of the reach considered. Also, this model shows that the location of the maximum shear stress is a function of the relative curvature (R/W) in the bends. By increasing R/W , the location of the maximum shear stress transfers to the downstream. This research shows that although construction of large dams converts the number, location, width, radius and length of bends, the location of the maximum shear stress in bends is dependent on the value of the relative curvature (R/W) of the bend.

The procedure for this research (using satellite images, RS, GIS and the CCHE2D model) for determining the location of erodible reaches in river can be applied to various rivers, and the results of this integrated method can help river engineers and designers protect river banks against erosion.

Acknowledgement

The authors of this manuscript would like to thank the managers and staffs of the civil engineering department and engineering faculty of Shahid Chamran University of Ahvaz for providing the facilities for this study.

REFERENCES

- Alauddin, M. – Tsujimoto, T. (2012)** *Optimum configuration of groyne for stabilization of alluvial rivers with fine sediments*. International Journal of Sediment Research, Vol. 27, No. 2, 158-167.
- Amiri-Tokaldany, E – Darby, S.E. – Tosswell, P. (2007)** *Coupling bank stability and bed deformation models to predict equilibrium bed topography in river bends*. Journal of Hydraulic Engineering-ASCE, Vol. 133, No. 10, 1167-1170.
- Avila, H. - Vargas, G. - Daza, R. (2014)** *Susceptibility analysis of river bank erosion based on exposure to shear stress and velocity combined with hydrologic and geomorphologic variables*. In World Environmental and Water Resources Congress, EWRI, American Society of Civil Engineering, ASCE. Portland, Oregon, USA.
- Bandyopadhyay, S. - Ghosh, K. - De, S.K. (2014)** *A proposed method of bank erosion vulnerability zonation and its application on the River Haora, Tripura, India*. Geomorphology, Vol. 224, 111-121.
- Brandt, S.A. (2000)** *Classification of geomorphological effects downstream of dams*. Catena, Vol. 40, No. 4, 375-401.
- Chang, H.H. (1983)** *Energy expenditure in curved open channels*. Journal of Hydraulic Engineering-ASCE, Vol. 109, No. 7, 1012-1022.
- Chang, H.H. (1985)** *Water and sediment routing through curved channels*. Journal of Hydraulic Engineering-ASCE, Vol. 111, No. 4, 644-658.
- Chang, H.H. (1994)** *Selection of gravel-transport formula for stream modeling*. Journal of Hydraulic Engineering-ASCE, Vol. 120, No. 5, 646-651.
- Chang, H.H. – Harrison, L.L. – Lee, W. – Tu, S. (1996)** *Numerical modeling for sediment-pass-through reservoirs*. Journal of Hydraulic Engineering-ASCE, Vol. 122, No. 7, 381-388.
- Chang, H.H. - Stow, D. (1989)** *Mathematical modeling of fluvial sand delivery*. Journal of Waterway, Port, Coastal, and Ocean Engineering –ASCE, Vol. 115, No. 3, 311-326.
- Constantine, J.A. – McLean, S.R. – Dunne, T. (2010)** *A mechanism of chute cutoff along large meandering rivers with uniform flood-plain topography*. Geological Society of America Bulletin, Vol. 122, No. 5-6, 855-869.
- Cramer, M.L. (2012)** *Stream habitat restoration guidelines*. Co-published by the Washington Departments of Fish and Wildlife, Natural Resources, Transportation and Ecology, Washington State Recreation and Conservation Office, Puget Sound Partnership, and the U.S. Fish and Wildlife Service, Olympia, Washington.
- Di Silvio, G. (2009)** *Simulating long-term river morphodynamics at watershed scale*. Canadian Journal of Civil Engineering, Vol. 36, No. 10, 1680-1688.
- Duan, J.G. – Wang, S.S.Y. – Jia, Y. (2001)** *The applications of the enhanced CCHE2D model to study the alluvial channel migration processes*. Journal of Hydraulic Research, Vol. 39, No. 5, 469-480.
- Ganasri, B.P. - Ramesh, H. (2016)** *Assessment of soil erosion by RUSLE model using remote sensing and GIS - A case study of Nethravathi Basin*. Geoscience Frontiers, Vol. 7, No.6, 953-961.
- Grimaud, J.L. – Chardon, D. – Metelka, V. – Beauvais, A. – Bamba, O. (2015)** *Neogene tectonic erosion fluxes and landform evolution processes from regional regolith mapping (Burkina Faso, West Africa)*. Geomorphology, Vol. 241, 315-330.
- Güneralp, İ. - Marston, R.A. (2012)** *Process–form linkages in meander morphodynamics: Bridging theoretical modeling and real world complexity*. Progress in Physical Geography, Vol. 36, No. 6, 718-746.
- Hasan, Z.A. – Lee, K.H. – Azamathulla, H.M. – Ghani, A.A. (2011)** *Flow simulation for lake Harapan using CCHE2D- a case study*. International Journal of Modelling and Simulation, Vol. 31, No. 1, 85-89.
- Haynes, H. - Pender, G. (2007)** *Stress history effects on graded bed stability*. Journal of Hydraulic Engineering-ASCE, Vol. 133, No. 4, 343-349.
- Ikeda, S. - Parker, G. (1989)** *River meandering*. the AGU Water Resources Monograph 12.
- Jang, E.K. – Ji, U. – Kwon, Y.S. – Yeo, W.K. (2013)** *Investigation for bed stabilization methods in the upstream channel of haman weir using CCHE2D model*. Journal of The Korean Society of Civil Engineers, Vol. 33, No. 6, 2211-2221.
- Jia, Y. – Wang, S.S.Y. (2001)** *CCHE2D: Two-dimensional hydrodynamic and sediment transport model for unsteady open channel flows over loose bed*. Technical Report No. NCCHE-TR-2001-1, School of Engineering, The University of Mississippi, University, MS 38677.
- Kean, J.W. – Kuhnle, R.A. – Smith, D. – Alonso, C.V. – Langendoen, E.J. (2009)** *Test of a method to calculate near-bank velocity and boundary shear stress*. Journal of Hydraulic Engineering-ASCE, Vol. 135, No. 7, 588-601.
- Khan, A.A. - Cadavid, R. - Wang, S.S.Y. (2000)** *Simulation of channel confluence and bifurcation using the CCHE2D model*. Proceedings of the Institution of Civil Engineers-Water and Maritime Engineering, Vol. 142, No. 2, 97-102.
- Kim, Y.S. - Jang, C.L. - Lee, G.H. - Jung, K.S. (2010)** *Investigation of flow characteristics of sharply curved channels by using CCHE2D model*. Journal of Korean Society of Hazard Mitigation, Vol. 10, No. 5, 125-133.
- Michalik, L.B.A. - Tekielak, T. (2013)** *The relationship between bank erosion, local aggradation and sediment transport in a small Carpathian stream*. Geomorphology, Vol. 191, 51-63.
- Nassar, M.A. (2011)** *Multi-parametric sensitivity analysis of CCHE2D for channel flow simulations in Nile River*. Journal of Hydro-Environment Research, Vol. 5, No. 3, 187-195.
- Nones, M. – Ronco, P. - Di Silvio, G. (2013)** *Modelling the impact of large impoundments on the Lower Zambezi River*. International Journal of River Basin Management, Vol. 11, No. 2, 221-236.
- Omran, M. (2008)** *New developments in predicting stage–discharge curves, velocity and boundary shear stress distributions in open channel flow*. Water and Environment Journal, Vol. 22, No. 2, 131-136.

- Patra, K.C. – Kar, S.K. – Bhattacharya, A.K. (2004)** *Flow and velocity distribution in meandering compound channels*. Journal of Hydraulic Engineering-ASCE, Vol. 130, No. 5, 398-411.
- Rüther, N. - Olsen, N.R.B. (2007)** *Modelling free-forming meander evolution in a laboratory channel using three-dimensional computational fluid dynamics*. Geomorphology, Vol. 89, No. (3-4), 308-319.
- Termini, D. (2015)** *Momentum transport and bed shear stress distribution in a meandering bend: Experimental analysis in a laboratory*. Advances in Water Resources, Vol. 81, 128-141.
- Thoman, R.W. - Niezgoda, S.L. (2008)** *Determining erodibility, critical shear stress, and allowable discharge estimates for cohesive channels: Case study in the Powder River basin of Wyoming*. Journal of Hydraulic Engineering-ASCE, Vol. 134, No. 12, 1677-1687.
- van den Berg, J.H. (1995)** *Prediction of alluvial channel pattern of perennial rivers*. Geomorphology, Vol. 12, No. 4, 259-279.
- Verhaar, P.M. - Biron, P.M. – Ferguson, R.I. – Hoey, T.B. (2008)** *A modified morphodynamic model for investigating the response of rivers to short-term climate change*. Geomorphology, Vol. 101, No. 4, 674-682.
- Wilcock, P.R. (1993)** *Critical shear stress of natural sediments*. Journal of Hydraulic Engineering-ASCE, Vol. 119, No. 4, 491-505.
- Yu, M. – Wei, H. – Liang, Y. – Hu, C. (2010)** *Study on the stability of noncohesive river bank*. International Journal of Sediment Research, Vol. 25, No. 4, 391–398.
- Zámolyi, A. - Székely, B. - Draganits, E. - Timár, G. (2010)** *Neotectonic control on river sinuosity at the western margin of the Little Hungarian Plain*. Geomorphology, Vol. 122, No. (3-4), 231-243.